



# HSV-NIS, an oncolytic herpes simplex virus type 1 encoding human sodium iodide symporter for preclinical prostate cancer radiovirotherapy

## Citation

Li, H, H Nakashima, T D Decklever, R A Nace, and S J Russell. 2013. "HSV-NIS, an oncolytic herpes simplex virus type 1 encoding human sodium iodide symporter for preclinical prostate cancer radiovirotherapy." *Cancer Gene Therapy* 20 (8): 478-485. doi:10.1038/cgt.2013.43. <http://dx.doi.org/10.1038/cgt.2013.43>.

## Published Version

doi:10.1038/cgt.2013.43

## Permanent link

<http://nrs.harvard.edu/urn-3:HUL.InstRepos:11855849>

## Terms of Use

This article was downloaded from Harvard University's DASH repository, and is made available under the terms and conditions applicable to Other Posted Material, as set forth at <http://nrs.harvard.edu/urn-3:HUL.InstRepos:dash.current.terms-of-use#LAA>

## Share Your Story

The Harvard community has made this article openly available.  
Please share how this access benefits you. [Submit a story](#).

[Accessibility](#)

## ORIGINAL ARTICLE

## HSV-NIS, an oncolytic herpes simplex virus type 1 encoding human sodium iodide symporter for preclinical prostate cancer radiovirotherapy

H Li<sup>1</sup>, H Nakashima<sup>2</sup>, TD Decklever<sup>3</sup>, RA Nace<sup>1</sup> and SJ Russell<sup>1,4</sup>

Several clinical trials have shown that oncolytic herpes simplex virus type 1 (oHSV-1) can be safely administered to patients. However, virus replication in tumor tissue has generally not been monitored in these oHSV clinical trials, and the data suggest that its oncolytic potency needs to be improved. To facilitate noninvasive monitoring of the *in vivo* spread of an oHSV and to increase its antitumor efficacy, the gene coding for human sodium iodide symporter (NIS) was incorporated into a recombinant oHSV genome and the corresponding virus (oHSV-NIS) rescued in our laboratory. Our data demonstrate that a human prostate cancer cell line, LNCap, efficiently concentrates radioactive iodine after the cells have been infected *in vitro* or *in vivo*. *In vivo* replication of oHSV-NIS in tumors was noninvasively monitored by computed tomography/single-photon emission computed tomography imaging of the biodistribution of pertechnetate and was confirmed. LNCap xenografts in nude mice were eradicated by intratumoral administration of oHSV-NIS. Systemic administration of oHSV-NIS prolonged the survival of tumor-bearing mice, and the therapeutic effect was further enhanced by administration of <sup>131</sup>I after the intratumoral spread of the virus had peaked. oHSV-NIS has the potential to substantially enhance the outcomes of standard therapy for patients with prostate cancer.

*Cancer Gene Therapy* (2013) **20**, 478–485; doi:10.1038/cgt.2013.43; published online 19 July 2013

**Keywords:** gene therapy; herpesvirus; prostatic neoplasms; radiotherapy; sodium iodide symporter

## INTRODUCTION

An estimated 241 740 new cases and 28 170 deaths due to prostate cancer occurred in the US during 2012.<sup>1</sup> Current treatment for metastatic human prostate cancer is palliative.<sup>2</sup> Oncolytic viruses have been examined extensively to treat various types of cancers in addition to human prostate cancers.<sup>3,4</sup> Oncolytic herpes simplex virus type 1 (oHSV-1) is attenuated through deletion of virulence factors to make it safe for administration to cancer patients.<sup>5</sup> As a DNA viral vector, oHSV-1 has superior potential to be engineered because of its ample genome space for transgene insertion and its wide tropism. Several preclinical and clinical trials have demonstrated that attenuated HSVs are safe,<sup>6,7</sup> but the trade-off is that their efficacy has been compromised. Although the replication of an oncolytic virus is crucial for its effectiveness, noninvasive monitoring of the intratumoral spread of oHSV-1 spreading in tumor-bearing patients has not been reported so far. Nevertheless, there is no doubt that the potency needs to be improved to get a better therapeutic effect from oHSVs in clinical use.

Several attempts have been made to enhance the anti-tumor potency of oncolytic viruses in various preclinical tumor models,<sup>8–12</sup> either by arming them with cytokine genes to boost the antitumor immune responses<sup>6,8,13–15</sup> or combining them with anticancer drugs<sup>16–18</sup> and/or radiotherapy.<sup>8,19</sup> However, off-target damage, restricted replication and incompetence to target smaller metastases need to be further addressed.<sup>20</sup>

Human sodium iodide symporter (NIS) is a membrane protein that transports iodide into thyroidal cells. NIS has been exploited as a marker gene for cancer gene therapy.<sup>21–24</sup> Several oncolytic viruses have been equipped with a NIS gene to facilitate

noninvasive *in vivo* monitoring<sup>25–30</sup> and potency enhancement by adding I-131 (<sup>131</sup>I).<sup>20,21,23,26,30,31</sup> In this paper, we report a novel NIS-expressing oHSV whose viral dynamics are not altered by the NIS transgene.

## MATERIALS AND METHODS

## Cell lines and virus rescue

Human prostate cancer cell lines LNCap, PC3 and DU145 were authenticated and obtained from ATCC (Manassas, VA, USA). Cells lines were passaged within 6 months of receiving from ATCC and characterized with DNA profiling by the cell bank. PCR was used to confirm that the cells were *Mycoplasma*-free before this study. Construction of oHSVs expressing NIS or firefly luciferase was carried out using HSVQuik technology as described previously.<sup>32,33</sup> The viruses were engineered to delete both copies of ICP34.5 and disrupt the ICP6 reading frame. NIS and luciferase transgenes were inserted under the control of cytomegalovirus promoter. The rescued viruses were amplified on Vero cells from a single plaque before preparation of working stocks. Supernatant and cell-associated virus progeny were harvested, subjected to three rounds of freeze–thawing, cleared of cell debris and then pelleted by centrifugation at 14 000 g for 1 h. Titers were determined by plaque assay on Vero cells. 3-(4,5-dimethylthiazol-2-yl)-5-(3-carboxymethoxyphenyl)-2-(4-sulfophenyl)-2H-tetrazolium (MTS) assays were used to measure the oncolytic activities of the rescued viruses in three human prostate cancer cell lines (Promega, Madison, WI, USA).

## Pertechnetate uptake assay and luciferase assay

To measure functional NIS expression, pertechnetate uptake assays were carried out as previously described.<sup>21,26,28</sup> Briefly, LNCap or Vero cells were

<sup>1</sup>Department of Molecular Medicine, Mayo Clinic, Rochester, MN, USA; <sup>2</sup>Department of Neurosurgery, Brigham and Women's Hospital, Harvard Medical School, Boston, MA, USA; <sup>3</sup>Department of Nuclear Medicine, Mayo Clinic, Rochester, MN, USA and <sup>4</sup>Division of Hematology, Mayo Clinic, Rochester, MN, USA. Correspondence: Dr SJ Russell, Department of Molecular Medicine, Mayo Clinic, 200 First Street SW, Rochester, MN 55905, USA. E-mail: sjr@mayo.edu

Received 6 June 2013; accepted 14 June 2013; published online 19 July 2013

infected with the indicated virus at a multiplicity of infection (MOI) of 1, 0.1, 0.01, 0.001 and 0.0001. After 24 or 72 h, technetium-99m as pertechnetate ( $^{99m}\text{TcO}_4$ ) was added to the medium. In control wells, 100 mM potassium perchlorate ( $\text{KClO}_4$ ) was added to block NIS activity. After 1-h incubation, the medium was removed and cells were washed twice. The remaining cells were resuspended in sodium chloride. Radioactivity was measured in a gamma-counter. The assays were performed in triplicate and the means plotted.

To measure firefly luciferase expression, the luciferase assay was performed according to the protocol provided by the manufacturer (Promega). The assay was performed with the whole-cell lysate, normalized to protein content and expressed as relative luciferase units.

## Animal studies

All animal experiments were performed in accordance with the guidelines of and with approval from the Institutional Animal Care and Use Committee of Mayo Foundation. Male athymic nu/nu mice (Charles River Laboratories, Frederick, MD, USA) aged 6–8 weeks were used for all the tumor studies.

For subcutaneous tumors, nude mice received a subcutaneous implant of  $1.5 \times 10^7$  LNCap cells mixed with Matrigel (BD Biosciences, San Jose, CA, USA) at a 1:1 ratio into the rear flank. When tumors reached an average volume of  $250 \text{ mm}^3$ , mice were administered phosphate-buffered saline (PBS) or the indicated virus by direct intratumoral injection or by tail vein injection ( $2 \times 10^6$  plaque-forming units (PFUs)). First day of therapy was designated as day 0. Tumor volume was calculated using the formula  $\text{length} \times \text{width}^2 \times 0.52$ . For radiovirotherapy, 1 mCi radioiodine  $^{131}\text{I}$  was administered intraperitoneally after viral injection at the time of peak  $^{99m}\text{TcO}_4$  uptake on the imaging studies.

## Computed tomography/single-photon emission computed tomography (CT/SPECT) imaging

Mice bearing LNCap tumors  $\geq 250 \text{ mm}^3$  were treated with PBS or the indicated virus. Imaging was performed as previously described using a high-resolution microSPECT/CT system (X-SPECT; Gamma Medica-Ideas, Northridge, CA, USA).<sup>22,23</sup> Briefly, 500 uCi  $^{99m}\text{TcO}_4$  was given 1, 3, 6, 9 and 12 days after oHSV-NIS treatment. Images were collected to monitor  $^{99m}\text{TcO}_4$  biodistribution 1 h after its injection and were analyzed using the

PMOD Biomedical Image Quantification and Kinetic Modeling Software (PMOD Technologies, Zurich, Switzerland). The level of  $^{99m}\text{TcO}_4$  uptake by the tumor was expressed as tumor activity in  $\mu\text{Ci}$  per tumor volume (cubic centimeter)."

## Autoradiography and immunohistochemical staining for oHSV

To confirm the expression of NIS in virus-treated tumors, we performed autoradiography using  $^{99m}\text{TcO}_4$  as previously described.<sup>22</sup> Similar to the imaging procedures, LNCap tumors were harvested at different time points after oHSV-NIS treatment. In all, 500 uCi  $^{99m}\text{TcO}_4$  was injected 1 h before tumor harvest. Serial tumor sections were obtained using a cryostat (Leica Microsystems, Buffalo Grove, IL, USA). For autoradiography, tumor sections were exposed to X-Omat radiographic (Carestream Health, Rochester, NY, USA) film in a darkroom and incubated overnight at  $4^\circ\text{C}$ . Sections for HSV staining were stored at  $-80^\circ\text{C}$ . Anti-HSV polyclonal antibody (Abcam, Cambridge, MA, USA) was applied to thawed sections after brief fixation with cold acetone. The staining was done using cell and tissue staining kit (R&D Systems, Minneapolis, MN, USA) according to the manufacturer's instructions.

## Statistical analysis

The *t*-test was used to analyze changes in cell killing and  $^{99m}\text{TcO}_4$  uptake. A *P*-value  $< 0.05$  was considered statistically significant. For survival analyses, Kaplan–Meier curves were plotted and compared using the log-rank test with GraphPad Prism 5.0 (GraphPad Software, La Jolla, CA, USA).

## RESULTS

### Generation and characterization of recombinant oHSV-NIS

The NIS gene has been previously inserted into several oncolytic viral genomes, including adenoviruses, measles virus, vesicular stomatitis virus and vaccine.<sup>29,30,34–37</sup> However, it was not known whether NIS expression could be compatible with oHSV-1. We therefore generated an oHSV-1 incorporating a NIS transgene driven by a cytomegalovirus promoter (oHSV-NIS). oHSV-Luc, the corresponding virus incorporating a firefly luciferase gene,

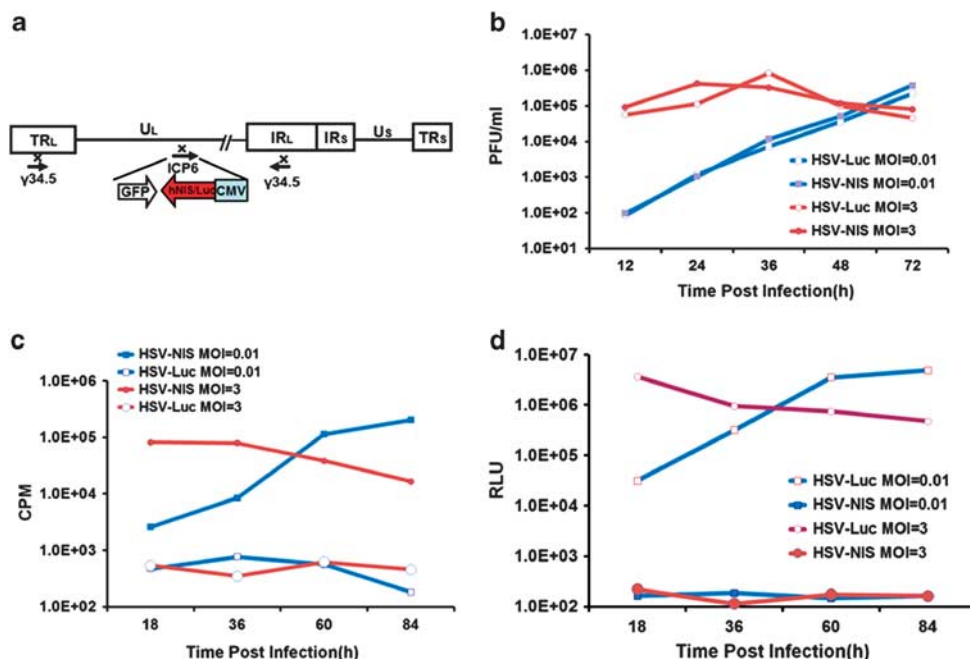


**Figure 1.** Rescue and characterization of recombinant viruses. (a) Schematic genome structures of oncolytic herpes simplex virus-sodium iodide symporter (oHSV-NIS) and oHSV-Luc. (b) oHSV-NIS and oHSV-Luc growth curves on Vero cells at different multiplicities of infection (MOIs). (c)  $^{99m}\text{TcO}_4$  uptake assays showing time course of functional NIS expression in oHSV-NIS-infected cells. (d) Luciferase assays showing time course of luciferase expression in oHSV-Luc-infected cells (MOIs of 1.0, 0.1 and 0.01). CMV, cytomegalovirus promoter/enhancer; CPM, counts per minute; GFP, green fluorescent protein; hNIS, human sodium iodide symporter; ICP6, infected cell protein 6; Luc, luciferase; PFU, plaque-forming units; RLU, relative luminescence unit.

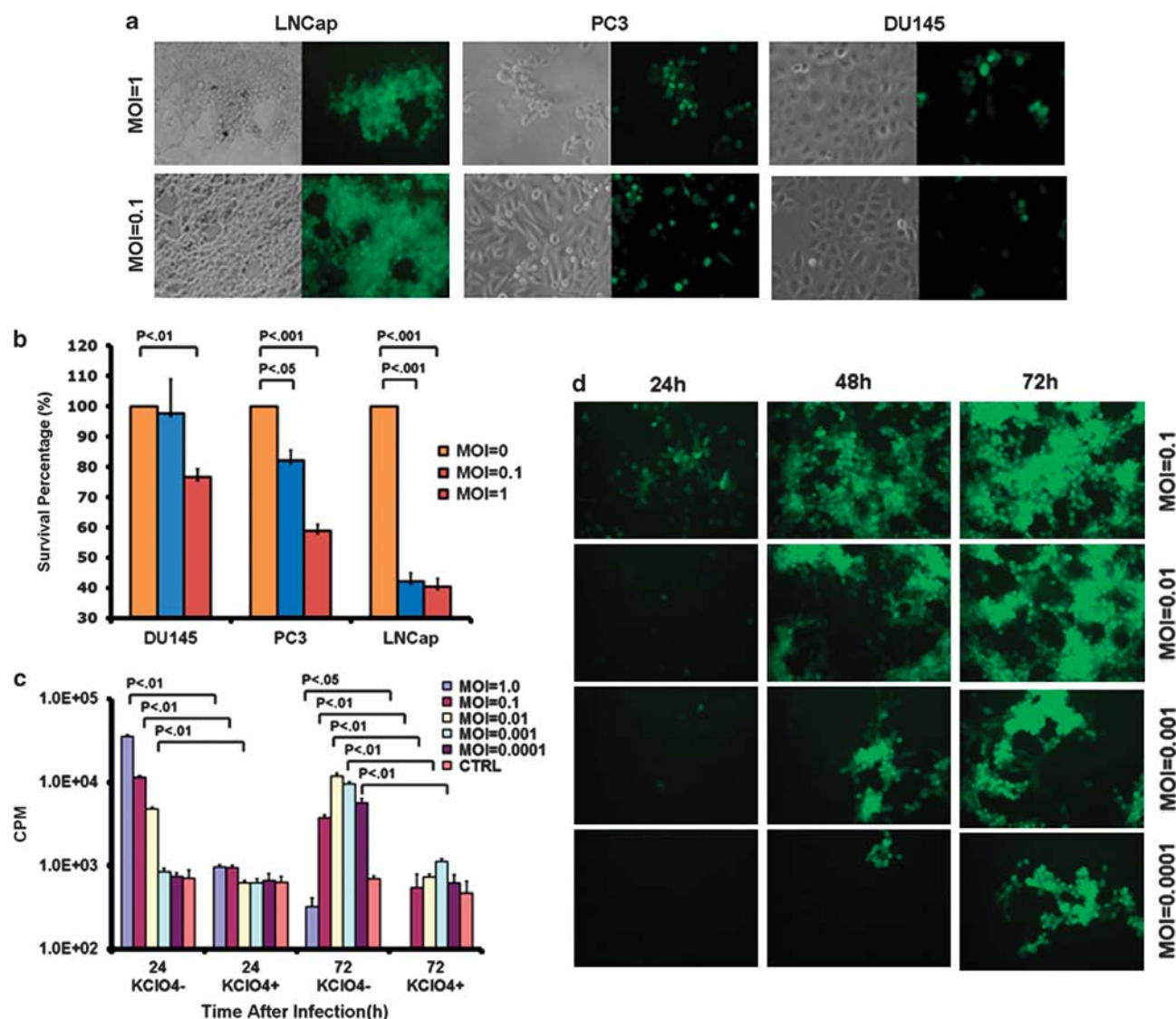


**Figure 2.** Infection of human prostate cancer cell lines by oncolytic herpes simplex virus-sodium iodide symporter (oHSV-NIS). Human prostate cancer cells LNCap, PC3 and DU145 were infected with oHSV-NIS. **(a)** Photographs taken under phase contrast and ultraviolet illumination 48 h after infection (multiplicity of infection (MOI) 0.1 or 1.0). **(b)** 3-(4,5-dimethylthiazol-2-yl)-5-(3-carboxymethoxyphenyl)-2-(4-sulfophenyl)-2H-tetrazolium (MTS) assay used to measure the killing ability of oHSV-NIS 72 h after infection (MOI 0.1 or 1.0). **(c)**  $^{99m}\text{TcO}_4$  uptake assay carried out to test NIS function in the presence or absence of its specific inhibitor potassium perchlorate ( $\text{KClO}_4$ ) at multiple indicated MOIs. The assay was read at 24 or 72 h after oHSV-NIS infection. **(d)** GFP expression in LNCap cells infected by oHSV-NIS at multiple indicated MOIs at 24, 48 and 72 h post infection.

was engineered and rescued similarly using the HSVQuik technology.<sup>11,32,38</sup> Figure 1a shows schematically the genome structures of oHSV-NIS and oHSV-Luc. The backbones of both viruses are from a first-generation oHSV-1, which was attenuated by deleting of both copies of ICP34.5 and disrupting ICP6. The growth kinetics of the viruses was compared after infection of Vero cells. Both oHSV-NIS and oHSV-Luc replicated similarly at MOI 0.1, 1 and 10 in Vero cells (Figure 1b). Expression of their respective transgenes was evaluated by testing radioactive iodine uptake or luciferase activity in the infected cell cultures. Thus,  $^{99m}\text{TcO}_4$  was concentrated in oHSV-NIS-infected Vero cells, with uptakes changing over time according to MOI (0.01 or 3), closely following the trend of the oHSV-NIS replication curve (Figure 1c). The luciferase assay showed a similar trend in oHSV-Luc-infected Vero cells (Figure 1d). The data indicate that both NIS and luciferase can be used as reporter genes to monitor oHSV replication *in vitro*.

#### Replication of oHSV-NIS in prostate cancer cells

To test the oncolytic activity of the new viruses, we infected human prostate cancer cell lines using oHSV-NIS or oHSV-Luc at MOI 0.1 and 1. Cytopathic effects were recorded 48 h after viral infection. LNCap cells were most permissive to oHSV-NIS infection, followed by PC3, then DU145 (Figure 2a). Loss of cell viability was evaluated by MTS assay (Figure 2b) and was in line with the green fluorescent protein expression data.

To further explore the potential of oHSV-NIS as an oncolytic virus for prostate cancer therapy, we focused our subsequent studies on the LNCap model. We first showed that oHSV-NIS can propagate efficiently in LNCap cells infected at MOIs ranging from 0.0001 to 0.1 by serial monitoring of green fluorescent protein expression (Figure 2c). NIS activity in the oHSV-NIS-infected cells was confirmed by  $^{99m}\text{TcO}_4$  uptake assays in the presence or absence of the perchlorate, a specific inhibitor of NIS-mediated  $^{99m}\text{TcO}_4$  uptake. Substantial NIS-specific  $^{99m}\text{TcO}_4$  uptake was



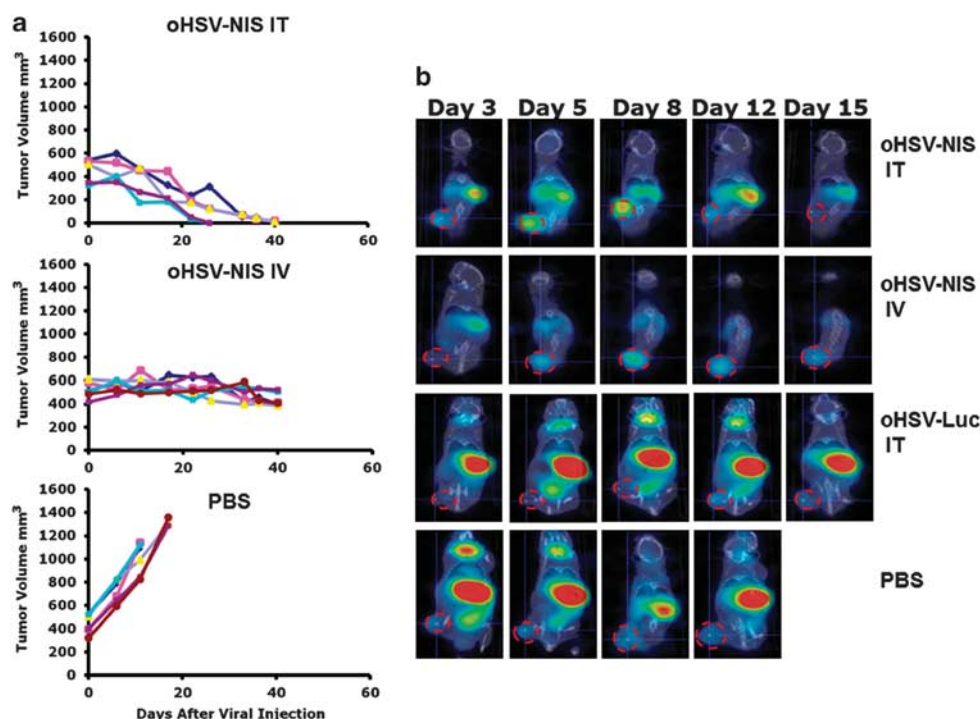


**Figure 3.** Antitumor activity of oncolytic herpes simplex virus-sodium iodide symporter (oHSV-NIS) in LNCap prostate cancer xenograft model. Male nude mice aged 6–8 weeks were implanted subcutaneously with LNCap cells and tumor-bearing mice were randomly assigned into three treatment groups. **(a)** Individual tumor growth curves are plotted for mice treated with intratumoral (IT) oHSV-NIS, intravenous (IV) oHSV-NIS and IT phosphate-buffered saline (PBS). **(b)** Three mice in each group were imaged using micro single-photon emission computed tomography/computed tomography at days 3, 5, 8, 12 and 15 after treatment. Images are shown for a single representative mouse from each group and for a control mouse treated IV with oHSV-Luc.

recorded in LNCap cells 24 h after oHSV-NIS infection at MOIs of 0.01, 0.1 and 1.0. Seventy-two hours after oHSV-NIS infection, the  $^{99m}\text{TcO}_4$  uptake had increased markedly in cells infected at very low MOIs of 0.001 and 0.0001, presumably a reflection of virus propagation (Figure 2d). The decreased 72-h  $^{99m}\text{TcO}_4$  uptake in LNCap cells infected at higher MOIs (0.1 and 1.0) is due to virus-mediated cell death. These data show that oHSV-NIS replication can be followed by monitoring NIS-mediated  $^{99m}\text{TcO}_4$  uptake in the infected cells.

#### Oncolytic efficacy of oHSV-NIS *in vivo*

For the evaluation of oncolytic efficacy of oHSV-NIS *in vivo*, human LNCap xenografts were established in male nude mice, and treatment was administered when tumor size reached  $>250\text{ mm}^3$ . oHSV-NIS ( $2 \times 10^6$  PFUs) was injected intratumorally or intravenously on day 0. Tumors continued to grow aggressively in control mice treated with PBS and met criteria for euthanasia within 3 weeks. Systemically administered oHSV-NIS stabilized tumor growth during the 40 days of observation while intratumoral oHSV-NIS led to complete tumor response in all the treated animals (Figure 3a).

In a parallel study, three mice per group were given intraperitoneal  $^{99m}\text{TcO}_4$  at specified time points after virus administration and were imaged with CT/SPECT (under inhalation anesthesia) 1 h later (Figure 3b). No  $^{99m}\text{TcO}_4$  uptake above background was detected in the tumors of PBS-treated mice. In contrast, robust uptake of  $^{99m}\text{TcO}_4$  was observed from day 3 after intratumoral injection of oHSV-NIS, increasing in intensity and peaking at day 8, then fading in parallel with tumor regression until it was no longer detectable by day 15. In systemically treated mice, the  $^{99m}\text{TcO}_4$  signal followed the same pattern, peaking on day 8 post-virus administration but was much weaker than the signal from the intratumoral-treated mice (Figure 3b). Radiotracer

uptakes of treated tumors at different time points after virus administration were calculated using PMOD Biomedical Image Quantification and Kinetic Modeling Software (Figure 4a). The quantification data showed that tumors treated intratumorally or intravenously with oHSV-NIS have significantly increased tracer uptakes compared with oHSV-Luc- or PBS-treated tumors. The peak Tc- $^{99m}\text{O}_4$  uptake following intratumoral oHSV-NIS therapy was around day 8, and the uptake decreased as the tumors regressed. However, tracer uptake by the intravenously oHSV-NIS-treated tumors made did increase above background until later time points, which may explain the lesser tumor response (Figure 3a). Several representatives immunohistochemical images are shown in Figure 4b to confirm that the HSV infection is solid and specific. These data suggested that the oHSV-NIS can replicate and spread in LNCap xenografts leading to efficient intratumoral concentration of  $^{99m}\text{TcO}_4$ .

To confirm the impression that oHSV-NIS was actively replicating and spreading in the LNCap xenografts, we performed immunohistochemical staining for HSV antigens and autoradiography for  $^{99m}\text{TcO}_4$  uptake on consecutive LNCap tumor sections. Tumor-bearing mice (10 per group) were given a single intratumoral or intravenous injection of oHSV-NIS. At specified intervals after virus administration,  $^{99m}\text{TcO}_4$  was administered by intraperitoneal injection to two mice from each group, and 1 h later, the mice were euthanized and their tumors were harvested, fixed in optimal cutting temperature and sectioned. Adjacent tumor sections were either exposed to radiographic film overnight or stained with polyclonal antibody against HSV, and the results were photographed for overlay. Substantial uptake of  $^{99m}\text{TcO}_4$  was detected day 5 after intravenous virus injection and peaked at day 8 (Figure 5). In the intratumoral-treated group, the tumor  $^{99m}\text{TcO}_4$  signal was detectable as early as day 3 after oHSV-NIS injection and peaked at day 8. The tumor signal was still detectable day 12 after virus administration independent of the route of

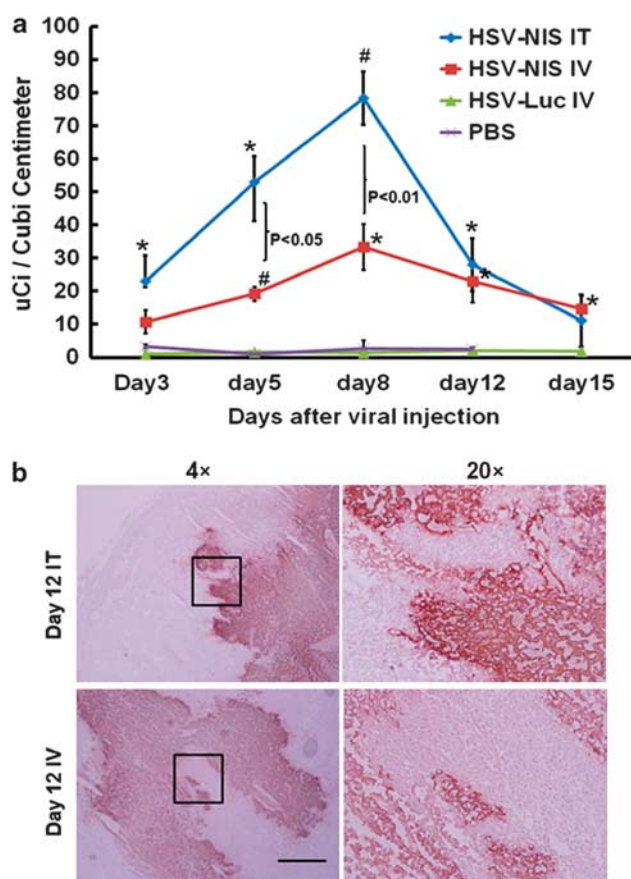


**Figure 4.** Replication and spreading of oncolytic herpes simplex virus-sodium iodide symporter (oHSV-NIS) in LNCap tumors *in vivo*. (a) Quantitative analysis of  $^{99m}\text{TcO}_4$  uptake in the LNCap prostate cancer xenograft model. LNCap tumors were treated and imaged as described in Figure 3b. The images at different time points were analyzed using the PMOD Biomedical Image Quantification and Kinetic Modeling Software. *P*-values were calculated to compare the uptakes from each group. \**P* < 0.05 vs phosphate-buffered saline (PBS) or HSV-Luc intravenous (IV); #*P* < 0.01 vs PBS or HSV-Luc IV. (b) Immunohistochemistry staining of oHSV infection. LNCap tumors were treated and imaged as described in Figure 3. Frozen sections were stained with a polyclonal anti-HSV antiserum. IT, intratumoral.

administration, but persisted slightly longer (to day 15) in the intravenous-treated group, becoming undetectable by day 22 (not shown). PBS-treated tumors showed no  $^{99m}\text{TcO}_4$  uptake above background. All oHSV-NIS-treated tumors stained positive for HSV antigens, and in all cases, the HSV staining co-localized with the autoradiographic signal. Some areas apparently infected by oHSV show no  $^{99m}\text{TcO}_4$  uptake, presumably because nonviable HSV-killed cells cannot concentrate the radioisotope, even if NIS positive. The poor correlation between signal intensity in these sections and tumor response (comparing intratumoral with intravenous delivery) should not be overinterpreted because the sections are a random sampling of the entire tumor.

#### Synergistic activity of oHSV-NIS with $^{131}\text{I}$ :radiovirotherapy

Human prostate cancer is a metastatic malignancy, and most prostate cancer deaths are a consequence of metastatic disease. For this reason, systemic administration of oncolytic viruses has been explored as a way of targeting small metastatic tumors.<sup>39,40</sup> However, as shown in Figure 3, intravenously injected oHSV-NIS could not eradicate large LNCap xenografts in the current study. Previously, NIS-expressing oncolytic viruses have been combined

with  $^{131}\text{I}$  radiotherapy to increase their antitumor potency (radiovirotherapy).<sup>21,23,26</sup> To determine whether  $^{131}\text{I}$  radiotherapy could enhance the efficacy of systemically administered oHSV-NIS, LNCap tumors were implanted as previously described and treated with oHSV-NIS or  $^{131}\text{I}$  alone or in combination. Control tumors were treated with PBS and continued to grow unabated. As previously, single-agent intravenous oHSV-NIS was able to stabilize tumor growth but was not curative. Intraperitoneal  $^{131}\text{I}$  administered day 7 after PBS had no effect on tumor growth, whereas  $^{131}\text{I}$  administered day 7 after oHSV-NIS led to substantial, often complete tumor regression. The combination of oHSV-NIS and radioiodine was therefore significantly superior to the activity of either agent alone (Figure 6a). oHSV-NIS-treated tumors started to regress very soon after  $^{131}\text{I}$  administration (Figure 6b), and this resulted in significant prolongation of overall survival (Figure 6c).

As an additional control, when oHSV-Luc was substituted for oHSV-NIS, subsequent administration of  $^{131}\text{I}$  did not lead to any enhancement of tumor response. Luminescence imaging was used to monitor the intratumoral amplification of the oHSV-Luc virus tail viral injection, and the luminescence signal did not increase following  $^{131}\text{I}$  administration (Figure 7), nor was there any acceleration of tumor regression seen when  $^{131}\text{I}$  was administered after intravenous oHSV-NIS (Figure 7).

## DISCUSSION

Oncolytic virotherapy is a promising new anticancer modality that can destroy tumor cells either by infecting them directly or by provoking an anticancer immune response.<sup>41</sup> Several oncolytic viruses are showing promise in ongoing clinical trials, but none have yet gained marketing approvals from the Food and Drug Administration, and there is still considerable room for improvement in their efficacy. Also, to date, there has been little insight gained from correlative studies as to the relative importance of intratumoral spread versus cross-priming of anticancer immunity in the clinical setting. This ability to noninvasively monitor the intratumoral expression of NIS-expressing oncolytic viruses is therefore an important development. NIS is a relatively large protein that is expressed abundantly in thyroid follicular cells where it traverses the cell membrane 13 times and serves to concentrate iodide, which is needed for thyroxine synthesis.<sup>42</sup> NIS has several advantages as a reporter gene because it is a self-protein; it is nonimmunogenic; it is nontoxic to the cells in which it is expressed; at 2 kb, the gene can be stably inserted into most viral vectors and NIS-compatible radioactive tracers such as  $^{123}\text{I}$  and  $^{99m}\text{TcO}_4$  are readily available for preclinical and clinical use in most medical centers.<sup>20,24,25,43</sup>

HSV is an appealing oncolytic platform for human use in part, because it naturally infects human populations and can reactivate repeatedly in a single infected host even in the face of a comprehensive antiviral immune response.<sup>5</sup> Several oHSV designs have been shown to be safe for administration in humans, including the ICP6/γ34.5 gene inactivated version used as a basis for oHSV-NIS. However, as with other oncolytic viruses which have been proven safe but not very effective in the clinic,<sup>4,44</sup> there is considerable interest in the generation of new oHSVs that will show greater antitumor potency in a clinical trial setting.<sup>6</sup> NIS gene insertion is one of the more interesting approaches that have been used to enhance the potency of other oncolytic viruses, allowing potency enhancement by administering a therapeutically active dose of  $^{131}\text{I}$ , a beta particle emitting radioisotope of iodine. This radiovirotherapy concept has been validated using different NIS-expressing oncolytic viruses in several different mouse tumor models.<sup>21,23,26,31,35</sup>

Here, for the first time, we have engineered a functional NIS transgene into a fully replication competent oHSV. Arming the virus with a NIS transgene allowed us to noninvasively monitor its intratumoral spread in living mice by serial SPECT/CT imaging of the biodistribution of  $^{99m}\text{TcO}_4$ , a readily available, clinically usable



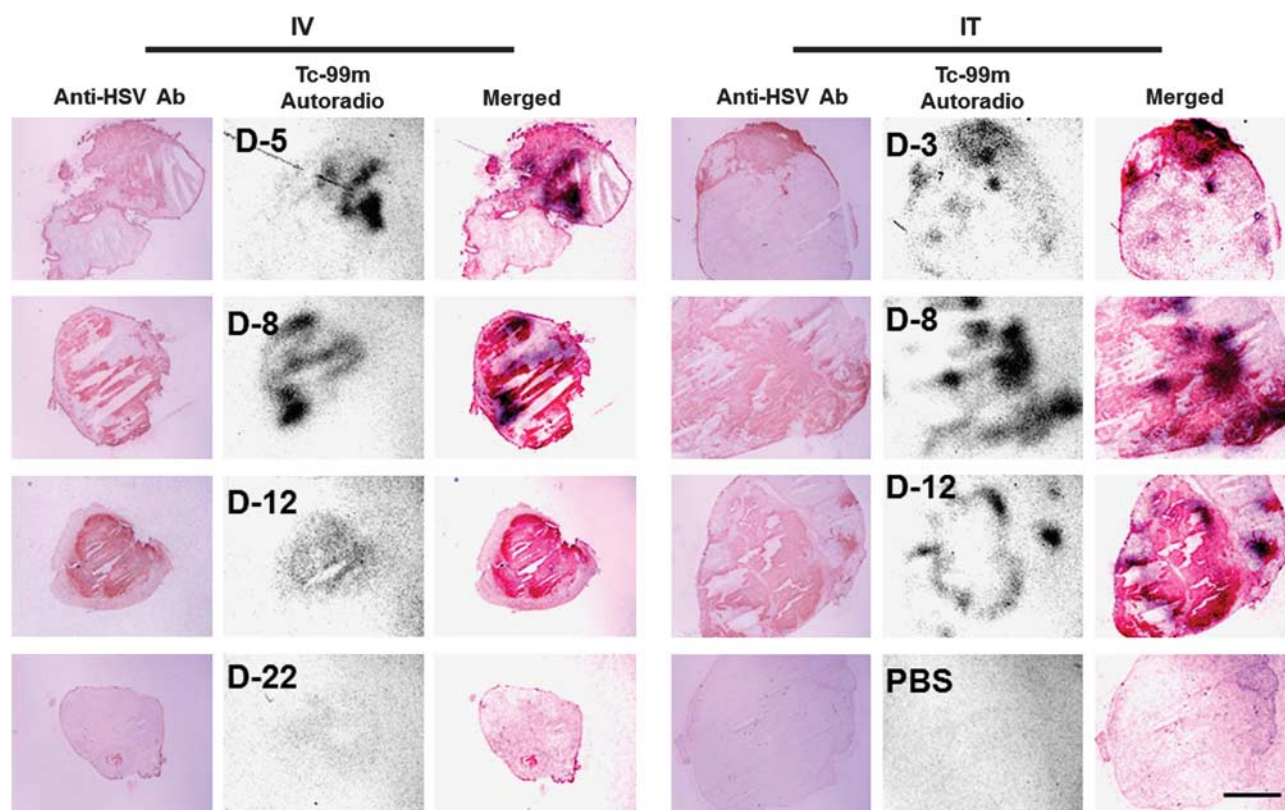


**Figure 5.** Co-localization of HSV staining and  $^{99m}\text{TcO}_4$  uptake in LNCap tumor sections from oncolytic herpes simplex virus-sodium iodide symporter (oHSV-NIS)-treated mice. Mice bearing LNCap tumors received oHSV-NIS by intratumoral (IT) or intravenous (IV) injection. A total of 500  $\mu\text{Ci}$   $^{99m}\text{TcO}_4$  was administered by intraperitoneal injection 1 h before euthanasia and tumor harvest. Frozen sections were stained with a polyclonal anti-HSV antiserum, and an adjacent section was exposed overnight to radiographic film. Photos were merged. Anti-HSV Ab, anti-HSV polyclonal antibody; autoradio, autoradiography; PBS, phosphate-buffered saline.

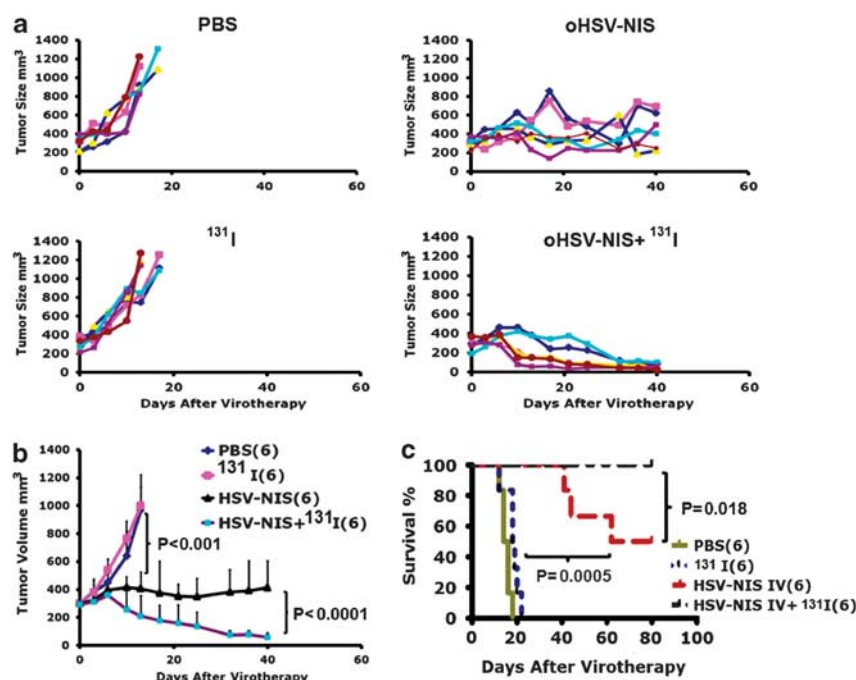


**Figure 6.** Radiovirotherapy with systemically administered oncolytic herpes simplex virus-sodium iodide symporter (oHSV-NIS) and radioiodine ( $^{131}\text{I}$ ) in the LNCap prostate cancer xenograft model. LNCap tumor-bearing mice were treated with phosphate-buffered saline (PBS) or oHSV-NIS (12 mice per group). Seven days later, half of the animals in each group received 1 mCi  $^{131}\text{I}$  by intraperitoneal injection. Tumor growth for individual mice treated with PBS, oHSV-NIS, PBS +  $^{131}\text{I}$  and oHSV-NIS +  $^{131}\text{I}$  in each group is plotted (a). Average tumor growth curves are plotted for all the groups (b). Corresponding Kaplan–Meier survival curves (c).

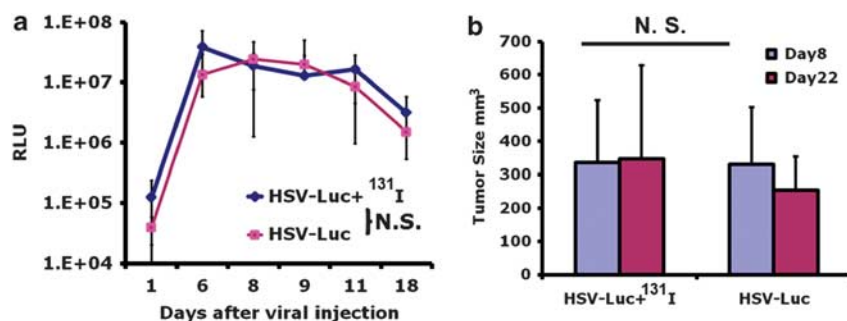


**Figure 7.** Radioiodine ( $^{131}\text{I}$ ) does not enhance the potency of oncolytic herpes simplex virus (oHSV)-Luc in the LNCap prostate cancer xenograft model. Twelve LNCap tumor-bearing mice were treated intravenously with oHSV-Luc. Seven days later, the animals were randomized into two groups, one of which received 1 mCi  $^{131}\text{I}$  by intraperitoneal injection. Serial measures of tumor luminescence (**a**) and tumor size (**b**) are shown. NS, not significant; RLU, relative luminescence unit.

gamma-emitting tracer with a short physical half-life of only 6 h. Systemic administration of oHSV-NIS was able to arrest the growth of human prostate cancer xenografts derived from the LNCap cell line but was not curative. However, when  $^{131}\text{I}$  was administered at the appropriate time (day 8) after systemic oHSV-NIS injection, the tumors (which were unresponsive to single agent  $^{131}\text{I}$ ) regressed completely.

Prostate cancer could be an appropriate target indication in which to demonstrate the oncolytic paradigm in humans.<sup>3,45,46</sup> Previously, an oncolytic adenovirus-expressing NIS was shown by  $^{99\text{m}}\text{TcO}_4$ -based SPECT/CT imaging to concentrate iodide in the virus-injected tumors of patients with prostate cancer.<sup>4</sup> Although the adenovirus used in this published clinical trial did not mediate tumor regressions,<sup>47</sup> the study did serve to establish the feasibility of exploiting NIS as a reporter gene for human oncolytic applications. We are hopeful that HSV will be able to replicate and spread faster than an oncolytic adenovirus in human prostate cancer. Moreover, as we have been able to demonstrate selective virus propagation in subcutaneous prostate tumor xenografts after systemic administration of oHSV-NIS, it is reasonable to propose that the virus be developed as a systemic therapy for patients with metastatic prostate cancer. The critical role of the virally encoded NIS transgene in these studies was confirmed by co-localization of HSV antigens with  $^{99\text{m}}\text{TcO}_4$  in LNCap tumor sections obtained from oHSV-NIS-treated mice.

Other groups are using radiovirotherapy for human prostate cancers, incorporating the NIS gene into the measles or adenovirus oncolytic platforms.<sup>3,4,35</sup> This is highly rational as there are major differences in the mechanisms of tumor cell targeting, intratumoral virus propagation and tumor cell killing for each of the viruses being evaluated. Parallel development of several virus platforms is therefore fully justified for the treatment of prostate cancer, and in each case, it is expected that the addition of the NIS transgene will be of significant value both to facilitate noninvasive monitoring of virus spread and to boost efficacy by administration of I-131. In this study, oHSV-expressing NIS could eradicate LNCap tumors rapidly with  $10^6$  pfus intratumoral injection, which has not been reported with other oncolytic viruses. However,  $^{131}\text{I}$  administration is known to cause off-target toxicity, primarily to thyroid and salivary glands. Although these toxicities are nonlethal and can be treated, for example, by thyroid hormone replacement therapy, several strategies are being developed to better protect these organs. In this study, there were no significant health changes observed among treated mice by the day the experiments terminated. Long-term toxicity of oHSV-NIS radiovirotherapy is being investigated.

Although it is widely used by for the evaluation of oncolytic viruses,<sup>3,4,35</sup> LNCap is considered to be a low-grade, androgen-responsive prostate cancer model. The results presented in this paper are therefore not necessarily predictive of activity in advanced metastatic prostate cancers, a question that is the subject of ongoing work.

The parental virus, oHSVQ which we used as a platform for the creation of HSV-NIS, was originally generated in the lab of Dr E Antonio Chiocca by deleting UL39 and both copies of the  $\gamma 34.5$  gene. The virus is therefore restricted in its replicative ability in noncancer cells, because it cannot combat the innate response to virus infection that leads to eIF2 $\alpha$  (enhanced initiation factor-2 $\alpha$ ) phosphorylation and translation shutoff.<sup>48</sup> The genetic structure of the HSV-NIS virus platform is therefore very similar to that of G207,<sup>49</sup> an HSV-1 mutant that was tested in clinical trials for humans with malignant glioma and shown to be safe up to the highest dose that could be tested, has been extensively studied and is known to spare non-malignant cells and tissues.<sup>50</sup> Also, oHSVQ-derived virus have previously been tested for neuroattenuation in mouse models and were found to be much safer than wild-type HSV.<sup>33</sup>

In summary, we report the construction and characterization of oHSV-NIS, a novel, NIS-expressing oHSV-1. We demonstrate when administered intravenously, the virus infects and selectively propagates in prostate cancer xenografts that are therefore able to concentrate  $^{99\text{m}}\text{TcO}_4$  and radioiodine, which provides a basis for noninvasive SPECT/CT imaging of intratumoral virus propagation and boosting of the antitumor response. HSV radiovirotherapy is a promising new approach to prostate cancer therapy and should be tested clinically.

## ABBREVIATIONS

CT, computed tomography; PFU, plaque-forming unit; HSV-1, herpes simplex virus type 1; IP, intraperitoneal, intraperitoneally; IT, intratumoral, intratumorally; IV, intravenous, intravenously; MOI, multiplicity of infection; NIS, sodium iodide symporter;  $^{131}\text{I}$ , sodium iodide I 131; SPECT, single-photon emission computed tomography;  $^{99\text{m}}\text{TcO}_4$ , technetium Tc 99m

## CONFLICT OF INTEREST

The authors declare no conflict of interest.

## ACKNOWLEDGEMENTS

We thank Dr E Antonio Chiocca for providing HSVQuik system. This work was supported by generous gifts from AI and Mary Agnes McQuinn, the Richard M Schulze Family Foundation, and the National Institutes of Health Grant R01CA100634, awarded to SJR.

## REFERENCES

- 1 ACS. Cancer facts and figures 2012 <http://www.cancer.org/acs/groups/content/@epidemiologysurveillance/documents/document/acspc-031941.pdf>.
- 2 D'Amico AV, Chen MH, de Castro M, Loffredo M, Lamb DS, Steigler A et al. Surrogate endpoints for prostate cancer-specific mortality after radiotherapy and androgen suppression therapy in men with localised or locally advanced prostate cancer: an analysis of two randomised trials. *Lancet Oncol* 2012; **13**: 189–195.



- 3 Fukuhara H, Homma Y, Todo T. Oncolytic virus therapy for prostate cancer. *Int J Urol* 2010; **17**: 20–30.
- 4 Barton KN, Stricker H, Brown SL, Elshaikh M, Aref I, Lu M et al. Phase I study of noninvasive imaging of adenovirus-mediated gene expression in the human prostate. *Mol Ther* 2008; **16**: 1761–1769.
- 5 Campadelli-Fiume G, De Giovanni C, Gatta V, Nanni P, Lollini PL, Menotti L. Rethinking herpes simplex virus: the way to oncolytic agents. *Rev Med Virol* 2011; **21**: 213–226.
- 6 Kaufman HL, Bines SD. OPTIM trial: a phase III trial of an oncolytic herpes virus encoding GM-CSF for unresectable stage III or IV melanoma. *Future Oncol* 2010; **6**: 941–949.
- 7 Geevarghese SK, Geller DA, de Haan HA, Horer M, Knoll AE, Mescheder A et al. Phase I/II study of oncolytic herpes simplex virus NV1020 in patients with extensively pretreated refractory colorectal cancer metastatic to the liver. *Hum Gene Ther* 2010; **21**: 1119–1128.
- 8 Harrington KJ, Hingorani M, Tanay MA, Hickey J, Bhide SA, Clarke PM et al. Phase I/II study of oncolytic HSV GM-CSF in combination with radiotherapy and cisplatin in untreated stage III/IV squamous cell cancer of the head and neck. *Clin Cancer Res* 2010; **16**: 4005–4015.
- 9 Russell SJ, Peng KW. The utility of cells as vehicles for oncolytic virus therapies. *Curr Opin Mol Ther* 2008; **10**: 380–386.
- 10 Todo T. Active immunotherapy oncolytic virus therapy using HSV-1. *Adv Exp Med Biol* 2012; **746**: 178–186.
- 11 Yoo JY, Haseley A, Bratasz A, Chiocca EA, Zhang J, Powell K et al. Antitumor efficacy of 34.5ENVE: a transcriptionally retargeted and "Vstat120"-expressing oncolytic virus. *Mol Ther* 2012; **20**: 287–297.
- 12 Lee CY, Bu LX, DeBenedetti A, Williams BJ, Rennie PS, Jia WW. Transcriptional and translational dual-regulated oncolytic herpes simplex virus type 1 for targeting prostate tumors. *Mol Ther* 2010; **18**: 929–935.
- 13 Pesonen S, Diaconu I, Kangasniemi L, Ranki T, Kanerva A, Pesonen SK et al. Oncolytic immunotherapy of advanced solid tumors with a CD40L-expressing replicating adenovirus: assessment of safety and immunologic responses in patients. *Cancer Res* 2012; **72**: 1621–1631.
- 14 Bortolanza S, Bunuales M, Otano I, Gonzalez-Aseguinolaza G, Ortiz-de-Solorzano C, Perez D et al. Treatment of pancreatic cancer with an oncolytic adenovirus expressing interleukin-12 in Syrian hamsters. *Mol Ther* 2009; **17**: 614–622.
- 15 Loeffler M, LeNegrate G, Krajewska M, Reed JC. Attenuated *Salmonella* engineered to produce human cytokine LIGHT inhibit tumor growth. *Proc Natl Acad Sci USA* 2007; **104**: 12879–12883.
- 16 Koski A, Raki M, Niksalmi P, Liikanen I, Kangasniemi L, Joensuu T et al. Verapamil results in increased blood levels of oncolytic adenovirus in treatment of patients with advanced cancer. *Mol Ther* 2012; **20**: 221–229.
- 17 Cheema TA, Kanai R, Kim GW, Wakimoto H, Passer B, Rabkin SD et al. Enhanced antitumor efficacy of low-dose Etoposide with oncolytic herpes simplex virus in human glioblastoma stem cell xenografts. *Clin Cancer Res* 2011; **17**: 7383–7393.
- 18 Pandha HS, Heinemann L, Simpson GR, Melcher A, Prestwich R, Errington F et al. Synergistic effects of oncolytic reovirus and cisplatin chemotherapy in murine malignant melanoma. *Clin Cancer Res* 2009; **15**: 6158–6166.
- 19 Harrington KJ, Melcher A, Vassaux G, Pandha HS, Vile RG. Exploiting synergies between radiation and oncolytic viruses. *Curr Opin Mol Ther* 2008; **10**: 362–370.
- 20 Touchefeu Y, Franken P, Harrington KJ. Radiovirotherapy: principles and prospects in oncology. *Curr Pharm Des* 2012; **18**: 3313–3320.
- 21 Dingli D, Peng KW, Harvey ME, Greipp PR, O'Connor MK, Cattaneo R et al. Image-guided radiovirotherapy for multiple myeloma using a recombinant measles virus expressing the thyroidal sodium iodide symporter. *Blood* 2004; **103**: 1641–1646.
- 22 Penheiter AR, Griesmann GE, Federspiel MJ, Dingli D, Russell SJ, Carlson SK. Pinhole micro-SPECT/CT for noninvasive monitoring and quantitation of oncolytic virus dispersion and percent infection in solid tumors. *Gene Therapy* 2011; **19**: 279–287.
- 23 Penheiter AR, Wegman TR, Classic KL, Dingli D, Bender CE, Russell SJ et al. Sodium iodide symporter (NIS)-mediated radiovirotherapy for pancreatic cancer. *Am J Roentgenol* 2010; **195**: 341–349.
- 24 Rajcecki M, Kangasmaki A, Laasonen L, Escutenaire S, Hakkarainen T, Haukka J et al. Sodium iodide symporter SPECT imaging of a patient treated with oncolytic adenovirus Ad5/3-Delta24-hNIS. *Mol Ther* 2011; **19**: 629–631.
- 25 Penheiter AR, Griesmann GE, Federspiel MJ, Dingli D, Russell SJ, Carlson SK. Pinhole micro-SPECT/CT for noninvasive monitoring and quantitation of oncolytic virus dispersion and percent infection in solid tumors. *Gene Therapy* 2012; **19**: 279–287.
- 26 Li H, Peng KW, Russell SJ. Oncolytic measles virus encoding thyroidal sodium iodide symporter for squamous cell cancer of the head and neck radiovirotherapy. *Hum Gene Ther* 2012; **23**: 295–301.
- 27 Gholami S, Haddad D, Chen CH, Chen NG, Zhang Q, Zanzonico PB et al. Novel therapy for anaplastic thyroid carcinoma cells using an oncolytic vaccinia virus carrying the human sodium iodide symporter. *Surgery* 2011; **150**: 1040–1047.
- 28 Li H, Peng KW, Dingli D, Kratzke RA, Russell SJ. Oncolytic measles viruses encoding interferon beta and the thyroidal sodium iodide symporter gene for mesothelioma virotherapy. *Cancer Gene Ther* 2010; **17**: 550–558.
- 29 Hakkarainen T, Rajcecki M, Sarparanta M, Tenhunen M, Airaksinen AJ, Desmond RA et al. Targeted radiotherapy for prostate cancer with an oncolytic adenovirus coding for human sodium iodide symporter. *Clin Cancer Res* 2009; **15**: 5396–5403.
- 30 Goel A, Carlson SK, Classic KL, Greiner S, Naik S, Power AT et al. Radioiodide imaging and radiovirotherapy of multiple myeloma using VSV(Delta51)-NIS, an attenuated vesicular stomatitis virus encoding the sodium iodide symporter gene. *Blood* 2007; **110**: 2342–2350.
- 31 Opyrchal M, Allen C, Iankov I, Aderca I, Schroeder M, Sarkaria J et al. Effective radiovirotherapy for malignant gliomas by using oncolytic measles virus strains encoding the sodium iodide symporter (MV-NIS). *Hum Gene Ther* 2012; **23**: 419–427.
- 32 Terada K, Wakimoto H, Tyminski E, Chiocca EA, Saeki Y. Development of a rapid method to generate multiple oncolytic HSV vectors and their in vivo evaluation using syngeneic mouse tumor models. *Gene Therapy* 2006; **13**: 705–714.
- 33 Kambara H, Okano H, Chiocca EA, Saeki Y. An oncolytic HSV-1 mutant expressing ICP34.5 under control of a nestin promoter increases survival of animals even when symptomatic from a brain tumor. *Cancer Res* 2005; **65**: 2832–2839.
- 34 Haddad D, Chen NG, Zhang Q, Chen CH, Yu YA, Gonzalez L et al. Insertion of the human sodium iodide symporter to facilitate deep tissue imaging does not alter oncolytic or replication capability of a novel vaccinia virus. *J Transl Med* 2011; **9**: 36.
- 35 Msaouel P, Iankov ID, Allen C, Aderca I, Federspiel MJ, Tindall DJ et al. Noninvasive imaging and radiovirotherapy of prostate cancer using an oncolytic measles virus expressing the sodium iodide symporter. *Mol Ther* 2009; **17**: 2041–2048.
- 36 Naik S, Nace R, Barber GN, Russell SJ. Potent systemic therapy of multiple myeloma utilizing oncolytic vesicular stomatitis virus coding for interferon-beta. *Cancer Gene Ther* 2012; **19**: 443–450.
- 37 Naik S, Nace R, Federspiel MJ, Barber GN, Peng KW, Russell SJ. Curative one-shot systemic virotherapy in murine myeloma. *Leukemia* 2012; **26**: 1870–1878.
- 38 Hardcastle J, Kurozumi K, Dmitrieva N, Sayers MP, Ahmad S, Waterman P et al. Enhanced antitumor efficacy of vasculostatin (Vstat120) expressing oncolytic HSV-1. *Mol Ther* 2010; **18**: 285–294.
- 39 Varghese S, Rabkin SD, Nielsen GP, MacGarvey U, Liu R, Martuza RL. Systemic therapy of spontaneous prostate cancer in transgenic mice with oncolytic herpes simplex viruses. *Cancer Res* 2007; **67**: 9371–9379.
- 40 Sova P, Ren XW, Ni S, Bernt KM, Mi J, Kiviat N et al. A tumor-targeted and conditionally replicating oncolytic adenovirus vector expressing TRAIL for treatment of liver metastases. *Mol Ther* 2004; **9**: 496–509.
- 41 Russell SJ, Peng KW, Bell JC. Oncolytic virotherapy. *Nat Biotechnol* 2012; **30**: 658–670.
- 42 Dingli D, Cascino MD, Josic K, Russell SJ, Bajzer Z. Mathematical modeling of cancer radiovirotherapy. *Math Biosci* 2006; **199**: 55–78.
- 43 Myers RM, Greiner SM, Harvey ME, Griesmann G, Kuffel MJ, Buhrow SA et al. Preclinical pharmacology and toxicology of intravenous MV-NIS, an oncolytic measles virus administered with or without cyclophosphamide. *Clin Pharmacol Ther* 2007; **82**: 700–710.
- 44 Galanis E, Okuno SH, Nascimento AG, Lewis BD, Lee RA, Oliveira AM et al. Phase I-II trial of ONYX-015 in combination with MAP chemotherapy in patients with advanced sarcomas. *Gene Therapy* 2005; **12**: 437–445.
- 45 Spitzweg C, Dietz AB, O'Connor MK, Bergert ER, Tindall DJ, Young CY et al. In vivo sodium iodide symporter gene therapy of prostate cancer. *Gene Therapy* 2001; **8**: 1524–1531.
- 46 Boland A, Ricard M, Opolon P, Bidart JM, Yeh P, Filetti S et al. Adenovirus-mediated transfer of the thyroid sodium/iodide symporter gene into tumors for a targeted radiotherapy. *Cancer Res* 2000; **60**: 3484–3492.
- 47 Barton KN, Stricker H, Elshaikh MA, Pegg J, Cheng J, Zhang Y et al. Feasibility of adenovirus-mediated hNIS gene transfer and 131I radioiodine therapy as a definitive treatment for localized prostate cancer. *Mol Ther* 2011; **19**: 1353–1359.
- 48 Chou J, Chen JJ, Gross M, Roizman B. Association of a M(r) 90,000 phosphoprotein with protein kinase PKR in cells exhibiting enhanced phosphorylation of translation initiation factor eIF-2 alpha and premature shutoff of protein synthesis after infection with gamma 134.5- mutants of herpes simplex virus 1. *Proc Natl Acad Sci USA* 1995; **92**: 10516–10520.
- 49 Mineta T, Rabkin SD, Yazaki T, Hunter WD, Martuza RL. Attenuated multi-mutated herpes simplex virus-1 for the treatment of malignant gliomas. *Nat Med* 1995; **1**: 938–943.
- 50 Markert JM, Medlock MD, Rabkin SD, Gillespie GY, Todo T, Hunter WD et al. Conditionally replicating herpes simplex virus mutant, G207 for the treatment of malignant glioma: results of a phase I trial. *Gene Ther* 2000; **7**: 867–874.



This work is licensed under a Creative Commons Attribution-NonCommercial-NoDerivs 3.0 Unported License. To view a copy of this license, visit <http://creativecommons.org/licenses/by-nc-nd/3.0/>